



Self-electrochemiluminescent CdTe quantum dots: one-pot synthesis, characterization, and electrochemical properties

Ting-Ting Han¹ · Shou-Nian Ding¹

Received: 18 September 2017 / Revised: 10 November 2017 / Accepted: 22 November 2017 / Published online: 30 November 2017
© Springer-Verlag GmbH Germany, part of Springer Nature 2017

Abstract

A novel self-electrochemiluminescent (self-ECL) nanomaterial, CdTe quantum dots, was prepared by the one-pot method using 2-diethylaminoethanethiol hydrochloride (DEAET) as capping agent and co-reactant (CdTe@DEAET QDs). Effects of various experimental variables such as Cd-to-Te ratio, pH value, and DEAET-to-Cd ratio on the optical and electrochemical properties have been systematically investigated. The results indicate that the as-prepared CdTe QDs show excellent size-dependent optical and self-ECL properties under optimal conditions. Moreover, the successful preparation of CdTe@DEAT QDs with morphology and structure were characterized by TEM, XRD, FT-IR, and XPS in this work. All these results corroborate that this preparation method of QDs presents a simple and easily up-scalable method for large-scale production.

Keywords One-pot synthesis · Properties · CdTe@DEAET QDs · Self-electrochemiluminescence

Introduction

Currently, electrochemiluminescence (ECL) is becoming a powerful detection method in the analytical fields due to its high sensitivity, low background noise, and simple instrumentation [1–4]. Normally, the introduction of co-reactants into the ECL system is a popular method in those applications, resulting in the improvement of analytical performance and ECL signal [5–8]. Nevertheless, directly introducing the co-reactants into ECL system will have negative effects on ECL efficiency of the luminophores for further applications [9–12]. The first is volatile properties and biological toxicity of co-reactants such as tripropylamine. The second is the complicated ECL systems and the redundant analytical steps to some extent. The third is the energy loss caused by the co-reactants diffusion to the electrode surface.

In previous ECL systems, considerable researches have been reported on ECL applications of the luminophores based on the presence of co-reactants in the testing solution in order to better reduce ECL potential and improve ECL efficiency [13–15]. Recently, however, many efforts have been focused on how to enhance the reaction efficiency between the luminophores and corresponding co-reactants because the intramolecular or intracluster electron transfer is more efficient compared with the intermolecular reaction due to the shorter electron-transfer distance and minor energy loss [16–19]. For example, Zhou et al. have established self-enhanced ECL immunosensor based on the hollow Ru-SiO₂@PEI nanoparticles for NSE analysis by attaching co-reactant poly(ethylenimine) (PEI) onto Ru-SiO₂ nanoparticles through electrostatic interaction [16]. Carrara and co-workers have reported the synthesis and ECL behavior of a new covalently linked hybrid of Ru(bpy)₃²⁺ and co-reactant amine-rich nitrogen-doped carbon nanodots (NCNDs) by amidation reaction, which enhances ECL signal [17]. These materials are more advantageous to greatly enhance ECL efficiency. Nevertheless, the synthetic steps such as ligand exchange and amide reaction are relatively complicated and time consuming.

Herein, we directly synthesize water-soluble CdTe quantum dots (CdTe QDs) with good optical properties and efficient self-electrochemiluminescence (self-ECL) performances using 2-diethylaminoethanethiol hydrochloride (DEAET) as

Electronic supplementary material The online version of this article (<https://doi.org/10.1007/s10008-017-3845-3>) contains supplementary material, which is available to authorized users.

✉ Shou-Nian Ding
sding@seu.edu.cn

¹ Jiangsu Province Hi-Tech Key Laboratory for Biomedical Research, School of Chemistry and Chemical Engineering, Southeast University, Nanjing 211189, China

protecting agent (CdTe@DEAET QDs) by the one-pot synthesis (Fig. 1). Specifically, DEAET works as a stabilizer as well as a co-reactant to enhance ECL of CdTe QDs. Hence, the design avoids the addition of co-reactants into the solution and generates a strong self-ECL emission owing to an intra-QDs electron transfer reaction.

Experimental section

Reagents

DEAET was purchased from Sigma-Aldrich. Tellurium powder (Te) was obtained from XingTa Chemical Plant Co. Ltd. (Shanghai, China). Cadmium chloride hemipentahydrate ($\text{CdCl}_2 \cdot 2.5\text{H}_2\text{O}$) and Sodium borohydride (NaBH_4) were obtained from Sinopharm Chemical Reagents Co. Ltd. (Shanghai, China). Phosphate buffer solutions (PBS, pH 7.0–9.0, and 0.1 M) were prepared by varying the ratio of Na_2HPO_4 to NaH_2PO_4 . All other reagents were of analytical grade and were used without further purification. Double-distilled water was used throughout.

Apparatus

All electrochemical and ECL experiments were carried out in a conventional three-electrode cell with a modified glassy carbon working electrode (GCE, diameter 3 mm), a Pt wire counter electrode, and a saturated calomel electrode (SCE) as reference electrode. Electrochemical experiments were performed with a CHI 660E electrochemical workstation (Shanghai Chen Hua Instrument Co., Ltd.) and an MPI-ECL Analyzer (Xi'an Remax Electronic High-Tech Ltd.). The photomultiplier tube (PMT) was biased at 800 V, and the ECL response was determined in 0.1 M PBS (pH 8.0) with a scan rate of 100 mV s^{-1} . UV-Vis absorption spectra were recorded on a Shimadzu UV-2450 Spectrophotometer (Tokyo, Japan). All photoluminescence (PL) measurements with the excitation wavelength of 400 nm were performed using a FluoroMax-4 fluorescence spectrophotometer

(Horiba, USA). High-resolution transmission electron microscopy (HR-TEM) measurements were conducted on a JEM-2100 transmission electron microscope (JEOL Ltd.). A Bruker D8 diffractometer with Cu $K\alpha$ radiation was used to record the X-ray diffraction (XRD) patterns. Data were collected from $2\theta = 20\text{--}70^\circ$ at a scan rate of $0.03^\circ/\text{step}$. The FT-IR spectrum was obtained from a Nicolet 5700 (USA) IR spectrometer in the range of $400\text{--}4000 \text{ cm}^{-1}$. X-ray photoelectron spectroscopy (XPS) analysis was performed on a Thermo ESCALAB 250 X-ray photoelectron spectrometer. The ECL spectrum was measured by collecting the various ECL intensities based on typical cyclic voltammetry with band-pass filters at the wavelengths of 525, 550, 575, 600, 625, 650, 675, 700, 725, and 750 nm used in the detection system, and the PMT was biased at 900 V; afterward, the difference of the ECL intensity was plotted with the corresponding wavelength. A vortex mixer IKA MS3 digital was selected to mix the solution.

One-pot synthesis of water-soluble CdTe@DEAET QDs

CdTe QDs capped with DEAET were synthesized according to the literature with slight modifications [20]. Briefly, $\text{CdCl}_2 \cdot 2.5\text{H}_2\text{O}$ (0.4 mmol) and DEAET (0.94 mmol) were mixed in 40 mL of H_2O and the solution pH was adjusted to 5.5 by dropwise addition of 1.0 M NaOH solution with stirring. Then, 0.4 mL of 0.04 M freshly prepared NaHTe solution (produced by reaction of oxygen-free NaBH_4 solution with Te powder under N_2 atmosphere) was injected through a syringe into the Cd precursor solution at room temperature, and the crude material turned to red-brown immediately. The final molar ratio of $\text{Cd}^{2+}:\text{Te}:\text{DEAET}$ was 1:0.04:2.4. Then the solution was stirred vigorously and refluxed at 120°C . By controlling the heating time, CdTe cores with different sizes were obtained. The resulting products were precipitated by acetone for two times centrifugation at 11,000 rpm for 5 min. The purified CdTe QDs were re-dissolved in double-distilled water as stock solution and then kept under dark at 4°C for later use. At the same time, a series of CdTe QDs were prepared by

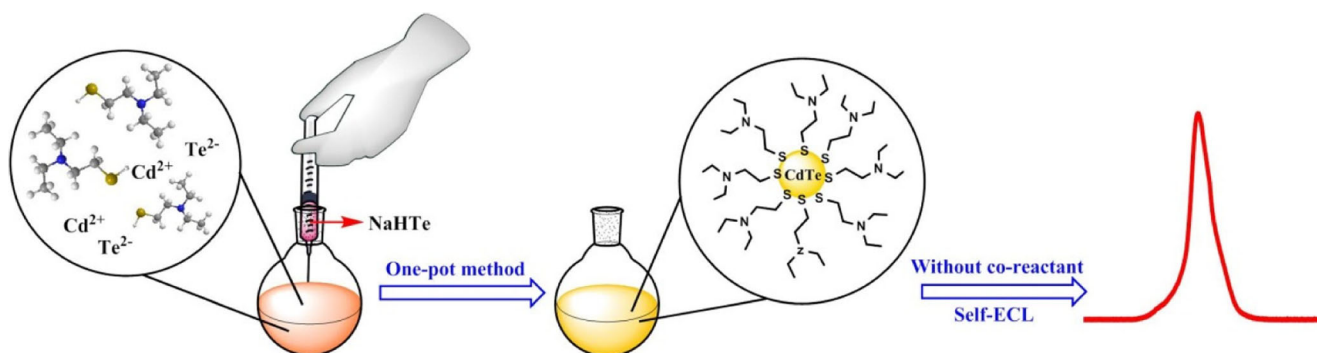


Fig. 1 Schematic illustrations of the preparation process for CdTe@DEAET QDs via one-pot method and its self-ECL behavior

changing experimental variables such as Cd-to-Te ratio, DEAET-to-Cd ratio, and pH value in the same way.

Standard procedures for ECL detection of QDs

A droplet of CdTe@DEAET QDs was dropped onto the glassy carbon electrode and dried in air at room temperature to obtain CdTe@DEAET QDs/GCE-modified electrodes. ECL measurements were carried out in 0.1 M PBS (pH 8.0) using CdTe@DEAET QDs/GCE as a working electrode. The applied working potential ranged from 0 to + 1.6 V, and the scan rate was 100 mV s⁻¹.

Results and discussions

Optical and electrochemical studies

Figure 2 shows the optical properties and corresponding ECL performances of CdTe QDs under the optimal conditions. With the proceeding of the QDs growth, both absorption peaks and the emission peaks of CdTe QDs shifted systematically to long wavelength due to the quantum size effect [21] (Fig. 2a, b). And the PL intensity was gradually increased under the same concentration, implying the increase of quantum yield of QDs. Figure 2c visually displayed photographs of CdTe@DEAET QDs taken under visible light and 365 nm UV light, respectively. Besides, the ECL intensity enhanced as the reaction time increased (Fig. 2d). This may be due to the

fact that the ECL intensity of CdTe QDs is related to their sizes and the ECL intensity of QDs increased with particle sizes [22, 23]. Next, we also found that the ECL onset potentials obviously shifted to the lower potential with the increase of the particle size (Table S1). Meanwhile, the size-dependent electrochemical behaviors of QDs have been reported in previous works owing to the quantum size effect [24, 25]. And we found that the oxidation potentials of CdTe@DEAET QDs from CV curves (Fig. S1) moved slightly in the negative direction as the QD size increased, which was agreed with ECL behavior. Furthermore, the ECL spectrum shows a main peak at 636 nm, very close to that of PL spectrum, meaning the surfaces of QDs have been largely passivated (Fig. S2). This was because DEAET may be more prone to the thermal decomposition, thus forming a layer of CdS-like shell on the surface of CdTe QDs [26]. This CdS-like shell might have effectively passivated the surface trap states, which enhanced the PL intensity and stability and ECL intensity of QDs [27].

Influence of Cd-to-Te molar ratio

To investigate the effect of the Te-to-Cd ratio, we fixed the DEAET-to-Cd molar ratio of 2.4:1, pH 5.5 and [Cd] = 10 mM. And then different amounts of NaHTe solution were added into obtained Cd-to-Te molar ratios from 10 to 30, respectively. With the same Te-to-Cd ratio, a series of samples were prepared in different hydrothermal time from 30 min to 10.5 h at intervals of 30 min. Figure 3 shows that the growth rate and the ECL intensities of CdTe QDs increased with the

Fig. 2 Temporal evolution of UV-vis spectra (a) and corresponding PL spectra (b) of CdTe@DEAET QDs during the reflux of the reaction solution with Cd:Te:DEAET molar ratios of 1:0.04:2.4, pH 5.5 and [Cd] = 10 mM. Photographs (c) of CdTe@DEAET QDs taken under visible light and 365 nm UV light, respectively. ECL signals (d) of CdTe@DEAET QDs during the reflux time (a–f: 0.5, 3.5, 6.5, 7.5, 9, and 10.5 h) of the reaction solution

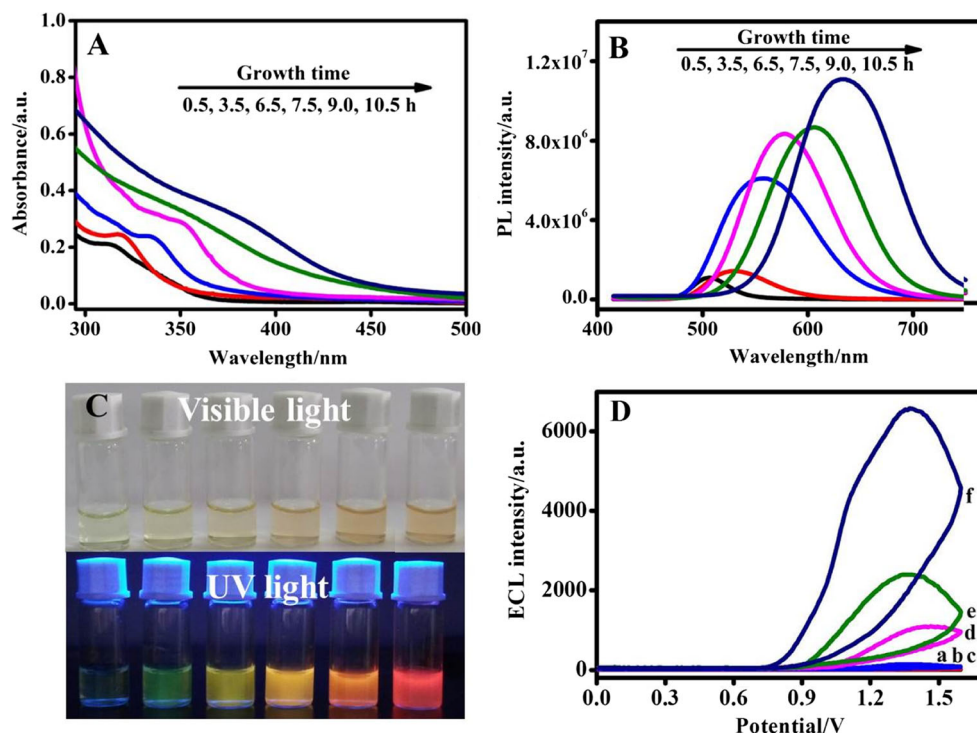
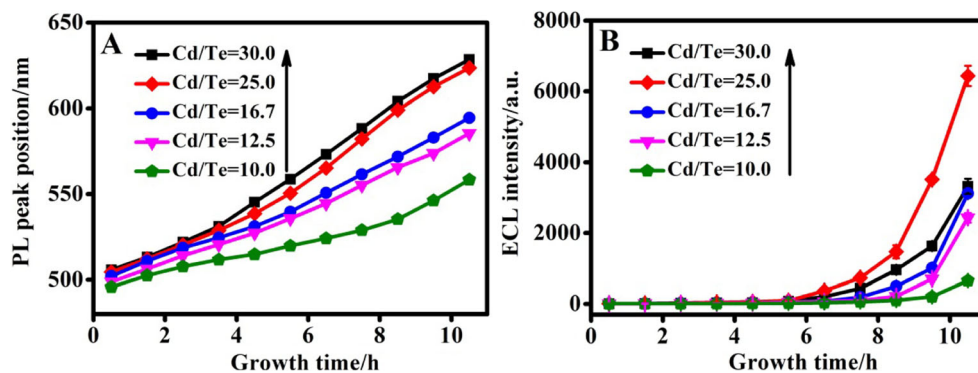


Fig. 3 Temporal evolution of the PL peak positions (a) and ECL signals (b) of CdTe@DEAET QDs growth under different Cd/Te molar ratios at pH 5.5



increase of Cd/Te ratio [28]. Moreover, we could find that the Cd/Te molar ratio of 25 got almost the highest growth rate and the greatest ECL signal. However, when the ratio was further increased to 30, the acceleration of QDs growth rate was almost negligible and the ECL intensity of CdTe QDs yet decreased. This was explained that high Cd-to-Te ratio made the growth turn to ripening period earlier because low Te concentration was beneficial to get bigger size nanocrystals with near-infrared emission, leading to the turbidity that appeared in the solution [29]. In view of the high quality and ECL performances of QDs, the Cd-to-Te ratio of 25 was chosen to conduct the following experiments.

Influence of pH value during the synthesis

To discuss the pH effect, we fixed the Cd:Te:DEAET ratio of 1:0.04:2.4, $[Cd] = 10$ mM, and changed the pH value of the reaction solution from 4.5 to 6.0. Figure 4 indicates that there was a huge acceleration of the CdTe growth rate when pH value changed from 4.5 to 5.5; this may be that the nature of the capping agent with alkaline functional group, namely, tertiary amine influences the particle growth of as-prepared CdTe@DEAET QDs [30]. Also, a significant enhancement of their corresponding ECL intensities could be ascribed to the size dependence of nanocrystals during the measurements [4, 23]. When pH value was 6.0, nevertheless, the growth rates and ECL signals of CdTe QDs obviously decreased compared with pH value of 5.5. However, we observed that the Cd-

DEAET solution became turbid after reflux at pH values of 6.5 and 7.0 and a precipitate appeared immediately, which may be due to the poor stability of CdTe@DEAET QDs in the synthesis condition, resulting in the poor quality of QDs [30]. Taking consideration of the greatest ECL signal and quality of CdTe QDs, we chose the pH value of 5.5 in this study.

Influence of DEAET-to-Cd molar ratio

Exploring the influence of ligand-to-Cd ratio, we fixed the Cd/Te ratio of 25, pH 5.5, $[Cd] = 10$ mM, and varied the DEAET/Cd molar ratio from 1.0 to 3.0. Figure 5 clearly describes that with the increase of DEAET/Cd ratio from 1.0 to 3.0, the growth rate and the ECL signals of QDs changed remarkably, especially after the growth time of 5.5 h. Moreover, there was no obvious difference in the growth rate when the DEAET-to-Cd ratio increased from 1.0 to 2.4, however, the ECL intensities of CdTe QDs enhanced significantly. These may be related to the quantum size effect and the concentrations of DEAET as co-reactants on the surface of QDs. While the DEAET/Cd ratio further increased to 3.0, the growth rate and ECL intensity of CdTe QDs increased slowly because too high ligand concentration was likely to suppress the growth of QDs. It was also noteworthy that for the lowest DEAET-to-Cd ratio of 1, the dispersion stability was significantly lower and particles started to precipitate within 1 week, probably owing to an incomplete surface passivation of QDs

Fig. 4 Temporal evolution of the PL peak positions (a) and ECL signals (b) of CdTe@DEAET QDs under different pH values of the reaction solution (pH 4.5, 5.0, 5.5, and 6.0) during the reflux with Cd:Te:DEAET molar ratios of 1:0.04:2.4

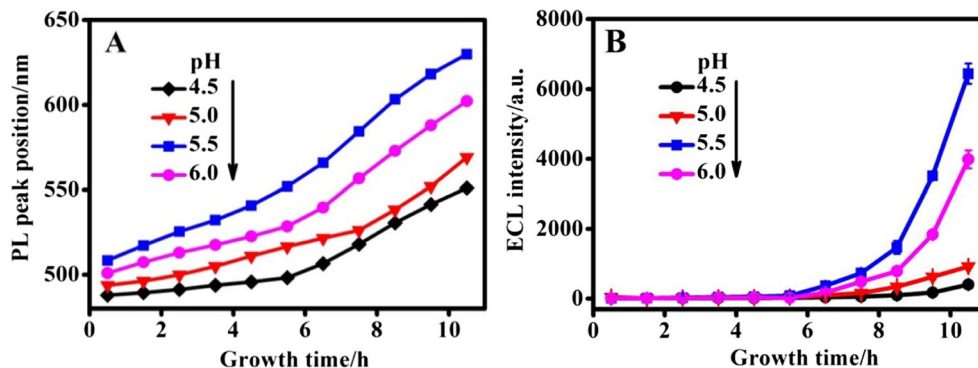
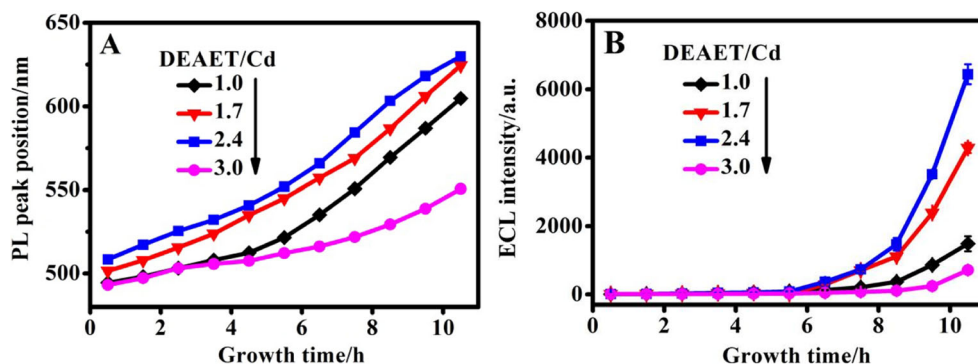


Fig. 5 Temporal evolution of the PL peak positions (a) and ECL signals (b) of CdTe@DEAET QD growth under varied DEAET-to-Cd molar ratios at pH 5.5



[27]. Therefore, we chose the DEAET-to-Cd ratio of 2.4 as the optimal parameter in the experiments.

CV and ECL performances of CdTe@DEAET QDs

Subsequently, we investigated the electrochemistry and ECL behaviors of CdTe@DEAET QDs prepared for 10.5 h under the optimized conditions (Fig. S3). As illustrated in Fig. 6, an obvious oxidation current and significant ECL emission can be observed in 0.1 M PBS at pH 8 without introducing co-reactants, indicating that DEAET as co-reactant indeed protected the surface of QDs and resulted in great ECL enhancement. This could be explained that the electron transfer distance between QDs and co-reactant DEAET was relatively shortened and thus significantly enhanced ECL efficiency of luminophores due to the intra-molecular or intra-QD electron transfer with the shorter electron-transfer path and minor energy loss [17, 31]. Only a slight change on the ECL intensity of CdTe@DEAET QDs was obtained when the sample was stored for 2 months, meaning the good stability of CdTe QDs (Fig. S4). Moreover, ECL intensity of CdTe QDs prepared by one-pot method is significantly enhanced compared with our previous work (Table S2) [18].

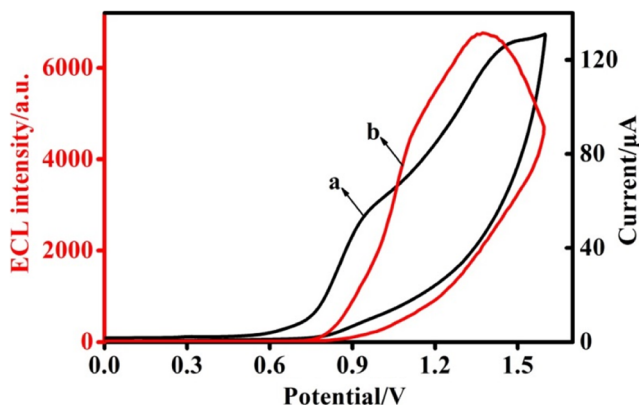


Fig. 6 The cyclic voltammogram (a) and ECL signal (b) of CdTe@DEAET QDs without adding co-reactants in 0.1 M PBS (pH 8.0). Scan rate, 100 mV s⁻¹

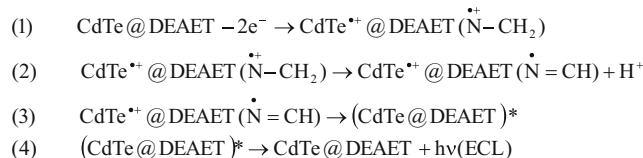
ECL mechanism of CdTe@DEAET QDs

According to the electrochemistry and ECL behavior of CdTe@DEAET QDs, we proposed the possible ECL mechanism of CdTe@DEAET QDs (Scheme 1). Briefly, both CdTe QDs and its superficial DEAET molecules as co-reactant are oxidized by electrode. Subsequently, the tertiary amines of DEAET become strong reductant after de-protonation, which reduces the oxidized CdTe QDs, analogous to the widely adopted Ru(bpy)₃²⁺-TPrA co-reactant pathway [32]. Afterwards, the activated CdTe QDs intermediates will generate ECL.

Morphology and structure characterization

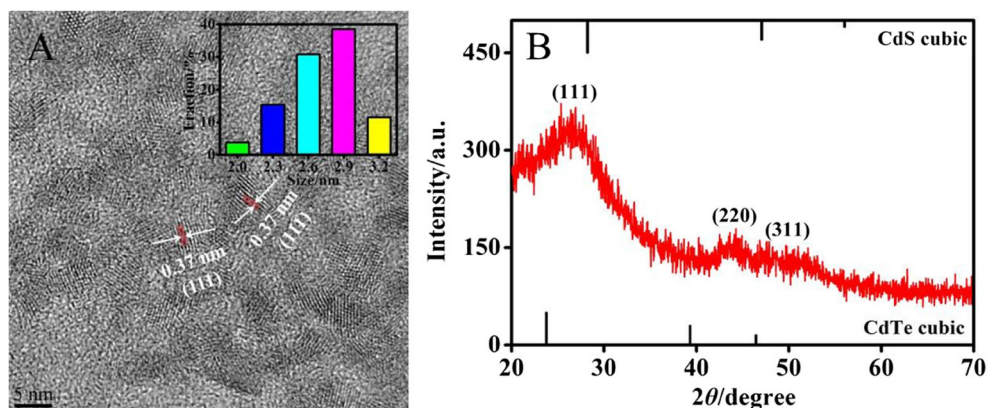
In order to characterize the morphology and structure of water-soluble CdTe@DEAET QDs, HR-TEM, XRD, FT-IR, and XPS characterization were carried out. The morphology of the CdTe@DEAET QDs was characterized using high-resolution transmission electron microscopy (HR-TEM). As shown in Fig. 7a, the HR-TEM image showed clearly that CdTe QDs are monodisperse and well-defined nanocrystals with the average diameter of 2.77 nm, close to the value of 2.80 nm resulting from the empirical equations [33]. Furthermore, The XRD results were compatible in the three cases and the diffraction peaks at 26.1°, 44.3°, and 51.3° were related to planes (111), (220), and (311), confirming that QDs have a zinc blende crystal structure like other thiol-capped CdTe QDs [28] (Fig. 7b). The lattice fringes of inter-planar distance of approximately 0.37 nm, determined by HR-TEM, and assigned to the (111) plane of CdTe QDs [26, 34].

Additionally, successful capping of DEAET to the surface of CdTe QDs is confirmed by FT-IR analysis (Fig. S5). The intense peak at near 3440 cm⁻¹ might arise from the



Scheme 1 Proposed ECL mechanism of CdTe@DEAET QDs

Fig. 7 The HR-TEM images (a) and XRD pattern (b) of CdTe@DEAET QDs with Cd:Te molar ratios of 1:0.08. The inset shows particle size distribution of the relative TEM

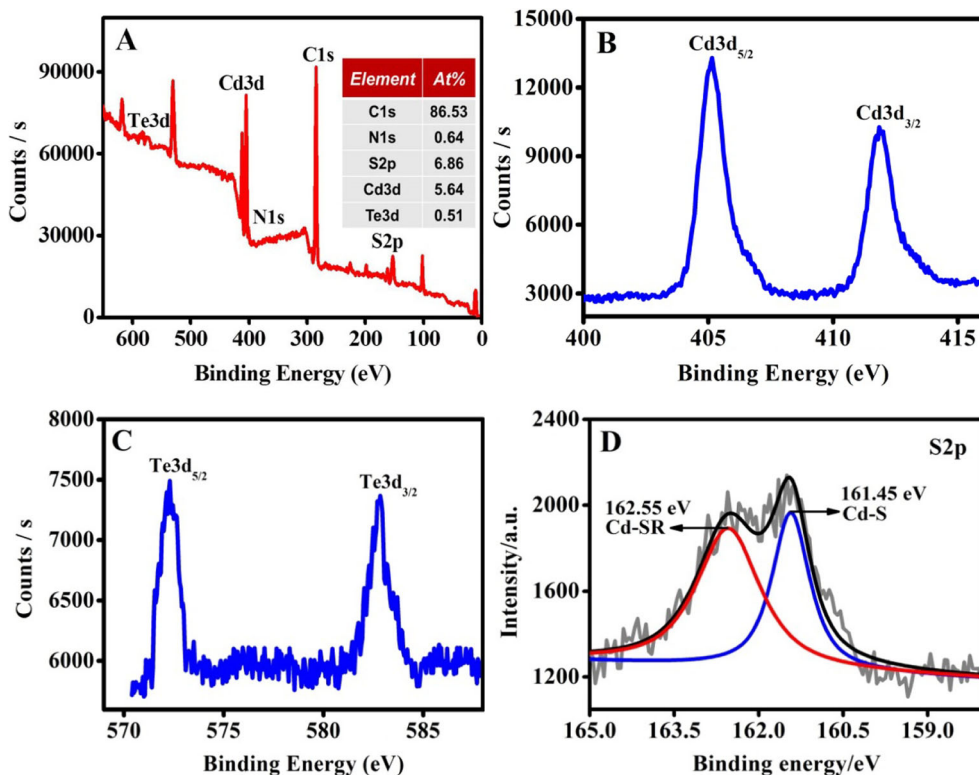


ammonium group of DEAET and H₂O molecules. The absorption bands at 2974, 2928, and 2852 cm⁻¹ can be attributed to the symmetric and asymmetric stretching vibration of -CH₂ and -CH₃ groups of the DEAET ligand, and the peaks at 1446 and 1379 cm⁻¹ may be assigned to the deformation vibration of -CH₂ and -CH₃ groups of DEAET [35, 36]. Moreover, the band at 1629 cm⁻¹ may arise from the bending modes of H₂O which could have been adsorbed from the atmosphere [37]. However, the peaks of the -SH groups on the surface of QDs at about 2530 cm⁻¹ disappeared due to the formation of covalent bonds between thiols and the Cd²⁺ on the surface of QDs.

Besides, further evidences on the surface structure of QDs can be obtained from the XPS analysis (Fig. 8). The characteristic peaks of C1s (284.6 eV), N1s (401.5 eV), S2p

(161.8 eV), Cd3d (Cd3d_{5/2} at 405.2 eV and Cd3d_{3/2} at 412.0 eV), and Te3d (Te3d_{5/2} at 572.3 eV and Te3d_{3/2} at 582.5 eV) were clearly observed (Fig. 8a–c), indicating the formation of CdTe QDs [7]. Furthermore, the inset showed that there exist Cd3d (5.64%), Te3d (0.51%), S2p (6.86%), N1s (0.64%), and C1s (86.53%) levels for DEAET-capped CdTe QDs (Fig. 8a, inset). The calculated constituent ratio of Cd to Te is 11.1:1, while the ratio of S to Te is 13.5:1. The ratio of Cd to Te is close to the theoretical value (12.5:1). The high ratio of S to Te may be attributed to the fact that the DEAET ligand together with the CdS-like shell is attached on the QDs. Additionally, the S2p peak was deconvoluted into two separate peaks at 161.45 and 162.55 eV corresponding to the typical characteristic peaks of Cd-S and Cd-SR, respectively,

Fig. 8 XPS spectra of a–d CdTe@DEAET QDs with Cd:Te molar ratios of 1:0.08. From (b) to (d), the spectra are Cd3d, Te3d, and S2p, respectively. The inset shows the element concentrations of CdTe@DEAET QDs



suggesting that the CdS-like shell is formed on the surface of CdTe QDs owing to the thermal decomposition of the capping ligands (Fig. 8d) [26].

Conclusions

In short, the water-soluble DEAET-capped CdTe QDs with unique self-ECL performance was successfully synthesized via facile one-pot method for the first time. Under the optimized experimental conditions (such as Cd-Te-DEAT ratio of 1:0.04:2.4, pH 5.5), the as-prepared CdTe QDs possessed fast growth rate, high-quality fluorescence, and enhanced self-ECL intensity in this work compared with our previous work. This synthesis of QD procedure holds a good potential for large-scale production and application and development of QD-based ECL.

Funding information This work was supported by the National Natural Science Foundation of China (21575022, 21535003), the National High Technology Research and Development Program (“863” Program) of China (2015AA020502), the Fundamental Research Funds for the Central Universities (2242016 K41055), Qing Lan Project, and A Project Funded by the Priority Academic Program Development of Jiangsu Higher Education Institutions (1107047002).

References

- Guo Z, Hao T, Duan J, Wang S, Wei D (2012) Electrochemiluminescence immunosensor based on graphene-CdS quantum dots-agarose composite for the ultrasensitive detection of alpha fetoprotein. *Talanta* 89:27–32. <https://doi.org/10.1016/j.talanta.2011.11.017>
- Hu L, Xu G (2010) Applications and trends in electrochemiluminescence. *Chem Soc Rev* 39(8):3275–3304. <https://doi.org/10.1039/b923679c>
- Wang L, Luo D, Qin D, Shan D, Lu X (2015) Cathodic electrochemiluminescence of a CdSe/ZnS QDs-modified glassy carbon electrode and its application in sensing of Pb²⁺. *Anal Methods* 7(4):1395–1400. <https://doi.org/10.1039/C4AY02304H>
- Zhang X, Ding SN (2016) General strategy to fabricate electrochemiluminescence sandwich-type nanoimmunosensors using CdTe@ZnS quantum dots as luminescent labels and Fe₃O₄@SiO₂ nanoparticles as magnetic separable scaffolds. *ACS Sens* 1(4):358–365. <https://doi.org/10.1021/acssensors.5b00242>
- Liu X, Ju H (2008) Coreactant enhanced anodic electrochemiluminescence of CdTe quantum dots at low potential for sensitive biosensing amplified by enzymatic cycle. *Anal Chem* 80(14):5377–5382. <https://doi.org/10.1021/ac8003715>
- Zhang X, Ding SN (2017) Graphite paper-based bipolar electrode electrochemiluminescence sensing platform. *Biosens Bioelectron* 94:47–55. <https://doi.org/10.1016/j.bios.2017.02.033>
- Zhao WW, Wang J, Zhu YC, Xu JJ, Chen HY (2015) Quantum dots: electrochemiluminescent and photoelectrochemical bioanalysis. *Anal Chem* 87(19):9520–9531. <https://doi.org/10.1021/acs.analchem.5b00497>
- Zou G, Ju H (2004) Electrogenerated chemiluminescence from a CdSe nanocrystal film and its sensing application in aqueous solution. *Anal Chem* 76(23):6871–6876. <https://doi.org/10.1021/ac049012j>
- Badocco D, Zanon F, Pastore P (2006) Use of Ru(bpy)₃²⁺/tertiary aliphatic amine system fast potential pulses electrochemiluminescence at ultramicroelectrodes coupled to electrochemical data for evaluating E° of amine redox couples. *Electrochim Acta* 51(28):6442–6450. <https://doi.org/10.1016/j.electacta.2006.04.029>
- Miao W, Choi JP, Bard AJ (2002) Electrogenerated chemiluminescence 69: the Tris(2,2′-bipyridine)ruthenium(II), (Ru(bpy)₃²⁺)/tri-n-propylamine (TPRA) system revisited—a new route involving TPRA⁺ cation radicals. *J Am Chem Soc* 124(48):14478–14485. <https://doi.org/10.1021/ja027532v>
- Pastore P, Badocco D, Zanon F (2006) Influence of nature, concentration and pH of buffer acid-base system on rate determining step of the electrochemiluminescence of Ru(bpy)₃²⁺ with tertiary aliphatic amines. *Electrochim Acta* 51(25):5394–5401. <https://doi.org/10.1016/j.electacta.2006.02.009>
- Liao N, Zhuo Y, Chai YQ, Xiang Y, Han J, Yuan R (2013) Reagentless electrochemiluminescent detection of protein biomarker using graphene-based magnetic nanoprobe and poly-L-lysine as co-reactant. *Biosens Bioelectron* 45:189–194. <https://doi.org/10.1016/j.bios.2013.02.005>
- Huang Y, Fang M, Zou G, Zhang B, Wang H (2016) Monochromatic and electrochemically switchable electrochemiluminescence of perovskite CsPbBr₃ nanocrystals. *Nano* 8:18734–18739
- Irkham, Watanabe T, Fiorani A, Valenti G, Paolucci F, Einaga Y (2016) Co-reactant-on-demand ECL: electrogenerated chemiluminescence by the in situ production of S₂O₈²⁻ at boron-doped diamond electrodes. *J Am Chem Soc* 138(48):15636–15641. <https://doi.org/10.1021/jacs.6b09020>
- Zhao M, Chen AY, Huang D, Zhuo Y, Chai YQ, Yuan R (2016) Cu nanoclusters: novel Electrochemiluminescence emitters for bioanalysis. *Anal Chem* 88(23):11527–11532. <https://doi.org/10.1021/acs.analchem.6b02770>
- Zhou L, Huang J, Yu B, You T (2016) A novel self-enhanced electrochemiluminescence immunosensor based on hollow Ru-SiO₂@PEI nanoparticles for NSE analysis. *Sci Rep* 6(1):22234. <https://doi.org/10.1038/srep22234>
- Carrara S, Arcudi F, Prato M, De Cola L (2017) Amine-rich nitrogen-doped carbon nanodots as platform for self-enhancing electrochemiluminescence. *Angew Chem* 56(17):4757–4761. <https://doi.org/10.1002/anie.201611879>
- Han TT, Dong H, Ren LL, Bao N, Wu W, Ding SN (2017) Self-electrochemiluminescence of CdTe nanocrystals capped with 2-diethylaminoethanethiol. *Chem Commun* 53(39):5388–5391. <https://doi.org/10.1039/C7CC01955F>
- Wang T, Wang D, Padelford WJ, Jiang J, Wang G (2016) Near-infrared electrogenerated chemiluminescence from aqueous soluble lipoid acid Au nanoclusters. *J Am Chem Soc* 138(20):6380–6383. <https://doi.org/10.1021/jacs.6b03037>
- Tang Z, Zhang Z, Wang Y, Glotzer SC, Kotov NA (2006) Self-assembly of CdTe nanocrystals into free-floating sheets. *Science* 314(5797):274–278. <https://doi.org/10.1126/science.1128045>
- Sheng Z, Han H, Hu X, Chi C (2010) One-step growth of high luminescence CdTe quantum dots with low cytotoxicity in ambient atmospheric conditions. *Dalton Trans* 39(30):7017–7020. <https://doi.org/10.1039/c002618b>
- Hua L, Han H, Zhang X (2009) Size-dependent electrochemiluminescence behavior of water-soluble CdTe quantum dots and selective sensing of L-cysteine. *Talanta* 77(5):1654–1659. <https://doi.org/10.1016/j.talanta.2008.09.061>
- Liu X, Jiang H, Lei J, Ju H (2007) Anodic electrochemiluminescence of CdTe quantum dots and its energy transfer for detection of catechol derivatives. *Anal Chem* 79(21):8055–8060. <https://doi.org/10.1021/ac070927i>

24. Poznyak SK, Osipovich NP, Shavel A, Talapin DV, Gao M, Eychmuller A, Gaponik N (2005) Size-dependent electrochemical behavior of thiol-capped CdTe nanocrystals in aqueous solution. *J Phys Chem B* 109(3):1094–1100. <https://doi.org/10.1021/jp0460801>
25. Li YC, Zhong HZ, Li R, Zhou Y, Yang CH, Li YF (2006) High-yield fabrication and electrochemical characterization of tetrapodal CdSe, CdTe, and CdSexTe1-x nanocrystals. *Adv Funct Mater* 16(13):1705–1716. <https://doi.org/10.1002/adfm.200500678>
26. Wang Q, Zhou X, Fang T, Liu P, Li X, Min X (2013) One-step growth of high-quality CdTe quantum dots via hydrothermal method and cytotoxicity evaluation. *Powder Technol* 247:81–86. <https://doi.org/10.1016/j.powtec.2013.07.007>
27. Myung N, Bae Y, Bard AJ (2003) Effect of surface passivation on the electrogenerated chemiluminescence of CdSe/ZnSe nanocrystals. *Nano Lett* 3(8):1053–1055. <https://doi.org/10.1021/nl034354a>
28. Wang Z, Li J, Liu B, Hu J, Yao X, Li J (2005) Chemiluminescence of CdTe nanocrystals induced by direct chemical oxidation and its size-dependent and surfactant-sensitized effect. *J Phys Chem B* 109(49):23304–23311. <https://doi.org/10.1021/jp055023k>
29. Zhang X, Wang L, Guo J, Yang W (2012) Stable water-dispersed CdTe nanocrystals dependent on stoichiometric ratio of Cd to Te precursor. *Chin J Chem* 30(5):1031–1039. <https://doi.org/10.1002/cjoc.201100672>
30. Gaponik N, Talapin DV, Rogach AL, Hoppe K, Shevchenko EV, Kornowski A, Eychmuller A, Weller H (2002) Thiol-capping of CdTe nanocrystals: an alternative to organometallic synthetic routes. *J Phys Chem B* 106(29):7177–7185. <https://doi.org/10.1021/jp025541k>
31. Wang H, Yuan Y, Zhuo Y, Chai Y, Yuan R (2016) Self-enhanced electrochemiluminescence nanorods of tris(bipyridine) ruthenium (II) derivative and its sensing application for detection of N-acetyl-β-D-glucosaminidase. *Anal Chem* 88(4):2258–2265. <https://doi.org/10.1021/acs.analchem.5b03954>
32. Miao W (2008) Electrogenerated chemiluminescence and its biorelated applications. *Chem Rev* 108(7):2506–2553. <https://doi.org/10.1021/cr068083a>
33. Yu WW, Qu L, Guo W, Peng X (2003) Experimental determination of the extinction coefficient of CdTe, CdSe, and CdS nanocrystals. *Chem Mater* 15(14):2854–2860. <https://doi.org/10.1021/cm034081k>
34. Miyake M, Inui H, Murase K, Hirato T, Awakura Y (2004) Comparison of microstructures of CdTe layers electrodeposited from basic ammoniacal and acidic sulfate electrolytes. *J Electrochem Soc* 151(3):C168–C175. <https://doi.org/10.1149/1.1643739>
35. Kuang R, Kuang X, Pan S, Zheng X, Duan J, Duan Y (2010) Synthesis of cysteamine-coated CdTe quantum dots for the detection of bisphenol A. *Microchim Acta* 169(1-2):109–115. <https://doi.org/10.1007/s00604-010-0323-3>
36. Testa G, Fontana L, Venditti I, Fratoddi I (2016) Functionalized platinum nanoparticles with surface charge triggered by pH: synthesis, characterization and stability studies. *Beilstein J Nanotechnol* 7: 1822–1828. <https://doi.org/10.3762/bjnano.7.175>
37. Thangadurai P, Balaji S, Manoharan PT (2008) Surface modification of CdS quantum dots using thiols-structural and photophysical studies. *Nanotechnology* 19(43):435708–435716. <https://doi.org/10.1088/0957-4484/19/43/435708>